Metallomics

PAPER

View Article Online
View Journal

Cite this: DOI: 10.1039/c8mt00225h

Cyclometallated Au(III) dithiocarbamate complexes: synthesis, anticancer evaluation and mechanistic studies†

Morwen R. M. Williams,[a] Benoît Bertrand, *[ab] David L. Hughes,[a] Zoë A. E. Waller,[c] Claudia Schmidt,[d] Ingo Ott,[d] Maria O'Connell,[c] Mark Searcey *[ac] and Manfred Bochmann *[a]

Received 3rd August 2018,
Accepted 18th September 2018

DOI: 10.1039/c8mt00225h

rsc.li/metallomics

A series of cationic mixed cyclometallated (C^N)Au(III) dithiocarbamate complexes has been synthesized in good yields [HC^N = 2-(*p*-*t*-butylphenyl)pyridine]. The crystal structure of $[(C^N)AuS_2CNEt_2]PF_6$ (**3**) has been determined. The cytotoxic properties of the new complexes have been evaluated *in vitro* against a panel of human cancer cell lines and healthy cells and compared with a neutral mixed (C^C)Au(III) dithiocarbamate complex (C^C = 4,4′-di-*t*-butylbiphenyl-2,2′-diyl). The complexes appeared to be susceptible to reduction by glutathione but were stable in the presence of *N*-acetyl cysteine. The potential mechanism of action of this class of compounds has been investigated by measuring the intracellular uptake of some selected complexes, by determining their interactions with higher order DNA structures, and by assessing the ability to inhibit thioredoxin reductase. The complexes proved unable to induce the formation of reactive oxygen species. The investigations add to the picture of the possible mode of action of this class of complexes.

Significance to metallomics

Gold(III) complexes are a current focus of research because of their promising anti-cancer properties. Many different structural types are being investigated; however, their mode of action remains largely obscure and difficult to predict. Here we report on the activity of cyclometallated gold(III) dithiocarbamate complexes. We show that the antiproliferative properties of these compounds can be correlated with their cellular uptake. Moreover, we demonstrate the ability of some of these complexes to selectively stabilize the non-canonical DNA G-quadruplex and i-motif structures. We also show that the complexes inhibit the enzyme thioredoxin reductase. On the other hand, the involvement of reactive oxygen species (ROS) in the cytotoxicity mechanism could be ruled out.

Introduction

Since the approval in the late 70's of *cis*-diamminodichloroplatinum(II) (cisplatin) for the treatment of various cancers including testicular, ovarian, prostate or lung cancers,[1] the field of metal-based anticancer drugs has grown rapidly. However, platinum drugs have several limitations, including resistances and heavy side effects affecting fast growing tissues.[2] This has led to a search for the possible replacement of platinum by other transition metals, such as iron,[3] copper,[4] ruthenium[5] or gold,[6] and promising results have been obtained. Organometallic complexes of gold in oxidation states +I and +III have attracted particular attention for anti-cancer purposes due to their high stability in physiological media and the ease of their derivatization. The evolution of the field has been regularly reviewed.[7] Cyclometallated Au(III) with (C^N), (N^N^C) or (C^N^C) ligands has been tested and shows activities up to the low-micromolar range.[8,9] Mono-cyclometallated (C^N)Au(III) complexes have appeared particularly interesting due to the large palette of (C^N) ligands available, including derivatives of *N*,*N*-dimethylbenzylamine,[10] phenylpyridine,[11] benzylpyridine,[12] or iminophosphorane.[13] A broad range of ancillary ligands is tolerated as well. Some representative examples are collected in Fig. 1.[14]

[a] School of Chemistry, University of East Anglia, Norwich, NR4 7TJ, UK. E-mail: benoit.bertrand@upmc.fr, m.searcey@uea.ac.uk, m.bochmann@uea.ac.uk
[b] Sorbonne Université, CNRS, Institut Parisien de Chimie Moléculaire (IPCM), F-75005 Paris, France
[c] School of Pharmacy, University of East Anglia, Norwich, NR4 7TJ, UK
[d] Institute of Medicinal and Pharmaceutical Chemistry, Technische Universität Braunschweig, Beethovenstrasse 55, D-38106 Braunschweig, Germany

† Electronic supplementary information (ESI) available. CCDC 1854835 (**3**). For ESI and crystallographic data in CIF or other electronic format see DOI: 10.1039/c8mt00225h

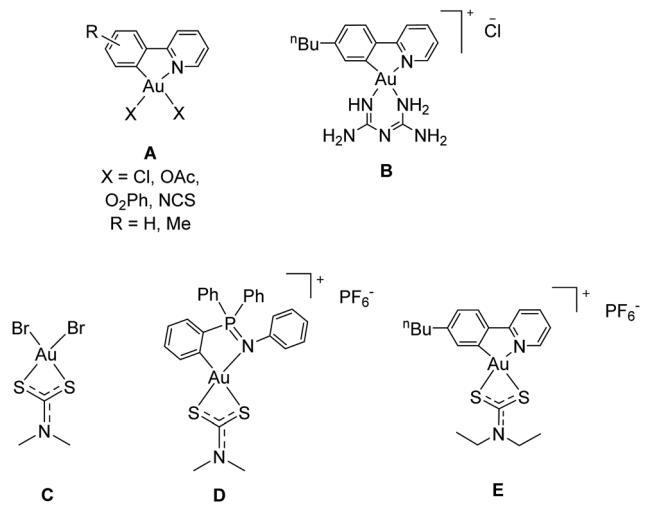

Fig. 1 Examples of (C^N) cyclometallated and dithiocarbamate Au(III) complexes investigated for anticancer purposes.

Although the mechanism of action of these complexes could not yet be fully elucidated,[6a] investigations have shown that cyclometallated (C^N)Au(III) complexes inhibit several enzymes such as cathepsin B and K,[12] thioredoxin reductase (TrxR)[8c,15] or poly(ADP)-ribose polymerase 1 (PARP-1).[16] Complex **B** bearing a highly hydrophilic biguanide ligand (Fig. 1) has been demonstrated to induce reticulum endoplasmic stress and to present anti-angiogenic effects at sub-cytotoxic concentrations.[17]

Dithiocarbamate (DTC) ligands are also well-known to efficiently stabilize Au(III) cations and have been widely used for making anticancer drug candidates (see for example Fig. 1 structures **C**–**E**).[7c] Complexes based on the scaffold **C** were highly active *in vitro* against several human cancer cell lines, induced the formation of reactive oxygen species (ROS), and triggered apoptosis *via* mitochondria-related pathways.[18,19] Inhibition of proteasomes by Au(DTC) complexes has also been demonstrated both *in vitro* and *in vivo*.[20]

The association of (C^N) cyclometallated ligands with dithiocarbamates ligands has been explored in Au(III)-based drug candidates using either iminophosphorane or phenylpyridine ligands (**D** and **E** in Fig. 1) and gave compounds with *in vitro* IC_{50} values in the low to submicromolar range against human cancer cells.[21,22] From a mechanistic point of view, (C^N)Au(DTC) complexes present several features in common with their pure DTC analogues, including cell death through both apoptosis and necrosis[21] and inhibition of proteasomes.[22] Furthermore, complex **E** has been demonstrated to have anti-angiogenic activity, similar to **B** which bears the same (C^N) ligand, and to inhibit deubiquitinases, enzymes regulating the ubiquitination of proteins.[22] However, the complete mechanism of action of that class of organogold complexes is far from fully elucidated.

Here we report the synthesis of a series of gold(III) compounds that combine the stabilisation by a cyclometallated (C^N) framework with dithiocarbamate (DTC) ligands, in an effort to probe their effect on a panel of human cancer cell lines *in vitro*, including lung cancer (A549), breast cancer (MCF-7 and MDA-MB-231), colon cancer (HCT-116) and leukaemia (HL60) cells and the normal human umbilical vein endothelial cells (HUVEC). We also explore their activity against different cellular targets associated with each class of compounds, namely the induction of ROS (dithiocarbamates), the interaction with non-canonical DNA structures (C^N chelates), and the inhibition of TrxR (typical of dithiocarbamates and some cyclometallated compounds).

Results and discussion

Synthesis and characterization

The (C^N) cyclometallated gold dichloride precursor **1** and the (C^C)Au(DTC) complex **7** were synthesized by previously reported methods.[22,24] An overnight reaction with sodium dialkyldithiocarbamate hydrate in methanol followed by the addition of aqueous potassium hexafluorophosphate or silver hexafluoroantimonate gave the cyclometallated dialkyl-dithiocarbamate complexes **2**–**6** in good yields (71–94%), as depicted in Scheme 1.

The ^{1}H NMR spectra of complexes **2**–**6** showed a significant downfield shift in the characteristic H^2 doublet signal from δ 9.71 to 8.40–8.78 ppm, as well as a downfield shift in the signal for H^{11} from δ 8.03 to 7.03–7.15 ppm, confirming the formation of the different complexes. The coordination of the dithiocarbamate

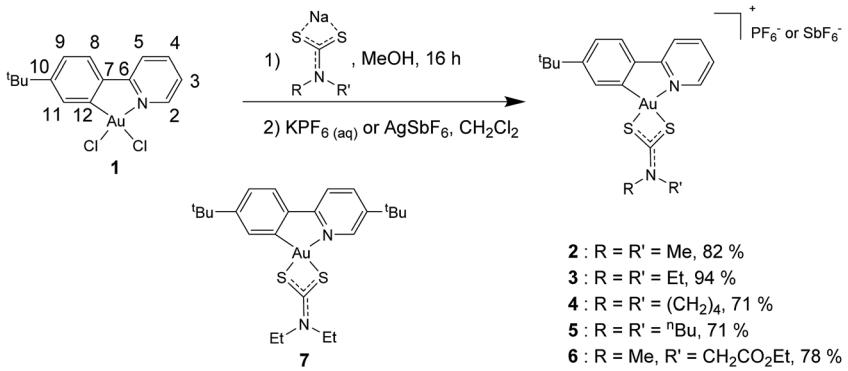

Scheme 1 Synthesis of the $[(C^N)Au(DTC)]^+$ complexes **2**–**6**, including the numbering scheme used for NMR signal assignments.

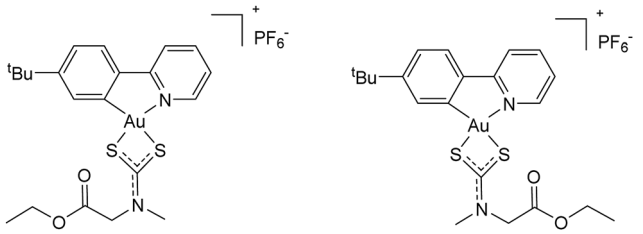

Fig. 2 Representation of the two structural isomers of **6**.

ligand was indicated by the observation of two inequivalent alkyl groups. The $C^{13}\{^1H\}$ NMR resonance for the NCS_2 carbon appeared between δ_C 190.4 and 198.7 ppm. Bands in the IR spectra between 1550 and 1579 cm^{-1} are attributed to the delocalised dithiocarbamate NCS_2 system. In the particular case of complex **6** bearing a non-symmetrically substituted DTC ligand based on sarcosine ethyl ester, the two possible isomers (Fig. 2) were observed in the ^1H NMR spectrum in a ratio of 1 : 0.8.

Slow vapour diffusion of diethyl ether into a concentrated acetonitrile solution of **3** gave crystals suitable for X-ray diffraction (Fig. 3). There are two independent cations in the unit cell, together with two PF_6^- anions and a single acetonitrile molecule. The two cations are essentially identical, each showing the square planar geometry typical of a gold(III) centre which is slightly distorted due to the narrow bite angles of the chelating (C^N) ligands (mean C–Au–N angle 80.75°) and the dithiocarbamates (mean S–Au–S angle 75.61°). Due to the different *trans* influences of C and N, the Au–S bond lengths are significantly different, with mean values 2.3953 and 2.2818 Å in the two molecules, similar to those found in related DTC complexes.[25]

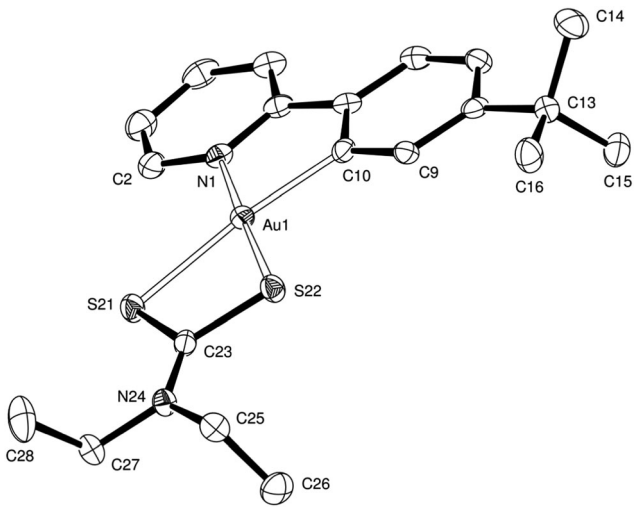

Fig. 3 Structure of one of the two cations $\mathbf{3}^+$. Hydrogen atoms, PF_6^- anions and the solvent molecule are omitted for clarity. Ellipsoids are shown at 50% probability. Selected bond distances [Å] and angles [°]: Au1–N1 2.061(3), Au1–C10 2.038(3), Au1–S21 2.3984(8), Au1–S22 2.2821(8), C10–Au1–N1 80.64(11), C10–Au1–S22 98.36(9), N1–Au1–S21 105.30(7), S22–Au1–S21 75.54(3), N1–Au1–S22 177.22(7), C10–Au1–S21 173.08(9), S21–C23–S22 111.47(17).

In vitro antiproliferative activity

Although the dithiocarbamate complexes **2–7** were poorly soluble in an aqueous cell culture medium, they were soluble enough in DMSO not to precipitate when diluted up to 100 μM in the aqueous culture medium with 1% DMSO. IC_{50} values for the six complexes were then determined on a panel of human cancer cell lines. These included solid tumour cell lines; lung adenocarcinoma cells (A549), breast adenocarcinoma (MCF-7 and MDA-MB-231) and human colon cancer (HCT-116) and suspension cells (promyelocytic leukaemia, HL60), as well as healthy Human Umbilical Vein Endothelial Cells (HUVEC) for comparison. Results were determined using a colorimetric MTS assay after 72 h of incubation in comparison to cisplatin (see Experimental part). The results are reported in Table 1.

Complexes **2–4** all showed similar cytotoxicity profiles, with high levels of cytotoxicity towards all the tested cell lines. The compounds were more active than the dichloro precursor **1** on all comparable cell lines. The two complexes presenting the shortest alkyl substituents on the dithiocarbamate ligand (**2** and **3**) showed an activity that was, respectively, 7 and 12 times higher than that of cisplatin towards A549 lung cancer and more than 15 times more active towards MCF-7 breast cancer and HL60 leukaemia cells. The complexes also showed more than twice the activity of cisplatin towards the colon cancer HCT-116 cells lines, while complex **3** was 15 times more active than cisplatin against the MDA-MB-231 metastatic breast cancer cells.

It was thought possible that an increase in lipophilicity of the complex could induce an increase in the cellular uptake. However, the more lipophilic pyrrolidine and dibutyl variants **4** and **5** were slightly less cytotoxic compared to **2** and **3**, although they still showed extremely promising levels of cytotoxicity in comparison to cisplatin. These results are in line with data reported on similar $[(C^N)Au(DTC)]^+$ complexes.[22] However, despite their promising anticancer activities all four complexes showed poor selectivity towards the Human Umbilical Vein Endothelial Cells (HUVEC), with IC_{50} values in the submicromolar range. Further tests on other healthy cell lines are needed for a more accurate conclusion as HUVEC are perhaps not the most reliable comparison, since they typically show a reduced sensitivity towards cisplatin.[29]

The sarcosine ethyl ester dithiocarbamate, complex **6** showed surprisingly low activities across the panel of cells, with IC_{50} values of more than 100 μM for A549, MCF-7, MDA-MB-231 and HCT-116. This could be due to poor cellular uptake as the complex is highly hydrophilic and therefore might struggle to cross the cell membrane. The complex also showed poor activity towards HL60, leukaemia cells, with an IC_{50} of 17.8 μM. In that case, the replacement of the two chlorido ligands by the sarcosine ester-based DTC ligand lead to the reduction in the antiproliferative activity of the Au(III) complex. However, this complex also showed the best selectivity profile of the new dithiocarbamates towards this cell line, (selectivity factor $S_{HL60/HUVEC}$ = 1.9).

The neutral (C^C) complex **7** also showed reduced cytotoxicity compared to its cationic (C^N) analogue **3**, particularly towards

Table 1 IC_{50} values for complexes **1–7** in comparison to cisplatin against different human cancer cell lines and healthy HUVEC cells after 72 h of incubation

	$IC_{50} \pm SD^a$ (μM)					
Complex	A549	MCF-7	HL60	HCT-116	MDA-MB-231	HUVEC
1[b]	43.6 ± 4.1	10.8 ± 3.5	6.0 ± 0.5	n.d.	n.d.	n.d.
2	4.6 ± 0.7	1.4 ± 0.3	0.2 ± 0.05	2.5 ± 0.3	8.6 ± 1.0	0.8 ± 0.04
3	2.9 ± 0.6	1.2 ± 0.2	0.2 ± 0.03	2.4 ± 0.4	1.9 ± 0.1	0.7 ± 0.02
4	10.8 ± 0.3	1.1 ± 0.03	1.4 ± 0.07	6.0 ± 0.4	3.0 ± 0.2	0.7 ± 0.05
5	5.3 ± 0.3	1.7 ± 0.04	0.8 ± 0.01	3.5 ± 0.3	3.1 ± 0.1	1.2 ± 0.2
6	>100	>100	17.8 ± 2.1	>100	>100	33.9 ± 5.4
7	>100	8.8 ± 0.2	1.9 ± 0.3	>100	>100	3.3 ± 0.03
Cisplatin	33.7 ± 3.7[c]	21.2 ± 3.9[c]	3.7 ± 0.3[c]	5.3 ± 0.2[d]	28.4 ± 0.1[d]	>100

[a] Mean ± the standard error of at least three independent experiments. [b] Values from ref. 26. [c] Values from ref. 27. [d] Values from ref. 28.

the HCT-116, MDA-MB-231 and A549 cells, although it was reasonably active towards MCF-7, breast cancer and HL60 leukaemia cells, (IC_{50} values of 8.8 and 1.9 μM respectively). Once again, the reduced activity could be due to reduced cellular uptake as the (C^C) cyclometallated ligand and the absence of a charge makes this complex very lipophilic.

Reaction with glutathione and *N*-acetyl cysteine

Many gold(III) complexes show only weak and reversible binding to DNA, which is the primary target of platinum-based drugs.[30] However, cytotoxic gold compounds have shown high reactivity towards model proteins. Consequently gold–protein interactions are generally thought to be responsible for the cytotoxic effects of these complexes and are regarded as their primary targets.[6c] Metal–protein binding sites generally involve the side chain residues of amino acids such as the thioether and thiolate sulphur atoms in L-methionine and L-cysteine, respectively.[31] Complex **2** as a representative for cationic $[(C^N)Au(DTC)]^+$ compounds was reacted with glutathione (GSH) and *N*-acetyl cysteine (NAC), which were selected as reliable models of target biomolecules. Although both GSH and NAC present the same thiol group, they have very different redox potentials, with the potential of NAC being 63 mV more positive than that of GSH. This makes NAC a weaker reductant compared to GSH.[32] On treating **2** at room temperature with GSH in a 1 : 1 mixture of DMSO-d_6 and D_2O, ^1H NMR spectroscopy showed the immediate splitting of the signal of the CH_2S group (multiplet at 2.75 ppm for GSH) into two signals (doublets of doublets at 2.8 and 3.1 ppm) characteristic of the formation of oxidized glutathione (GSSG) (Fig. 4A).[33] Although no signals for the complex could be seen due to its poor solubility in these solvents, the formation of a pale-yellow product was observed, which suggested reduction to a gold(I) species. This reduction of **2** by GSH could also be followed by UV/vis spectroscopy (Fig. 4B). Upon mixing a 1 mM solution of **2** in DMSO with 1 mM of GSH in H_2O, the characteristic ligand-to-metal charge-transfer (LMCT) band[34] of **2** at 350 nm disappeared, confirming that fast reduction occurred, as already observed for gold(III) complexes with bipyridyl ligands.[35] The appearance of a broad UV/vis band at 400–450 nm could also be tentatively attributed to a gold(I) species.[36] The same features could also be seen when other dithiocarbamate derivatives were reacted with GSH (Fig. S1–S5, ESI†).

The interaction of **2** and **3** with *N*-acetyl cysteine (NAC) was also investigated, using NAC as a model for thiol containing biomolecules. Boscutti *et al.* showed that $Au^{III}Br_2(DTC)$ complexes underwent a rapid multi-step reduction in the presence of NAC, during which NAC was oxidized to *N*-acetyl cystine (NACy) and gold(III) was reduced to gold(I), possibly AuBr, with release of dithiocarbamate.[33a] Both **2** and **3** were mixed at room temperature with NAC in CD_3CN, and the reaction was followed by ^1H NMR spectroscopy over a 48 h period (Fig. 5 and ESI,† Fig. S6). No reaction was observed for either complexes during this time. It was concluded that the presence of the cyclometallated (C^N) ligand rendered the system stable towards reduction by NAC. Indeed, we observed neither the disappearance of the SH signal (triplet at 1.8 ppm) nor a shift of the signal due to the CH_2S group typical of the oxidation of NAC.[33a] Thus it appears that Au(III) compounds associating cyclometallated and dithiocarbamate ligands present an intermediate redox stability between the pure dithiocarbamate and pure cyclometallated complexes. The presence of cyclometallated ligand improves the redox stability of the (DTC)Au(III) scaffold (stability in the presence of NAC), while on the other hand the DTC ligand decreased the stability of the Au(III) centre against reduction. This demonstrate the possibility for fine tuning the redox properties of Au(III) complexes through suitable ligand combinations.

Cellular uptake

Cellular uptake of drugs can have a significant influence on the cytotoxicity of prospective chemotherapeutic agents.[37] Inductively coupled plasma-mass spectrometry (ICP-MS) was used to quantify the amount of intracellular gold and determine whether the uptake of the dithiocarbamate complexes correlated with their cytotoxicity. Complexes **2** and **5** (the dimethyl and dibutyl variants) were selected as these represented, respectively, the shortest and longest alkyl substituents R in the $[(C^N)Au^{III}(S_2CNR_2)]^+$ series. The sarcosine ethyl ester variant **6** was selected because it showed extremely poor cytotoxicity towards all tested cell lines, together with **7**, the (C^C) diethyl dithiocarbamate, as it was charge-neutral and the only complex

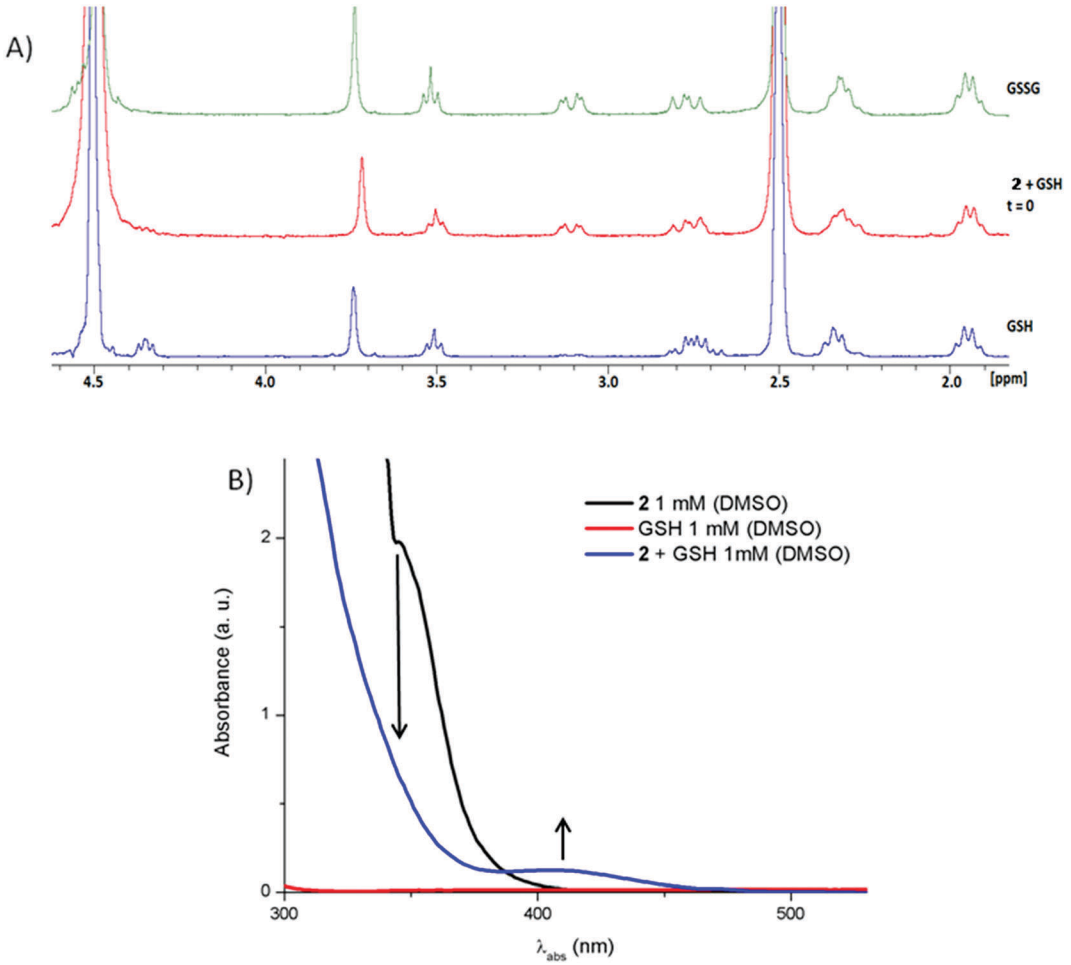

Fig. 4 (A) ^{1}H NMR spectra of a 1 : 1 mixture of **2** with GSH at room temperature, in comparison with the starting materials, GSH and GSSG (DMSO-d_6/D_2O 1 : 1). (B) UV/vis spectra of complex **2** (1 mM), GSH (1 mM) and a mixture of complex **2** and GSH (1 mM), (DMSO–H_2O 1 : 1).

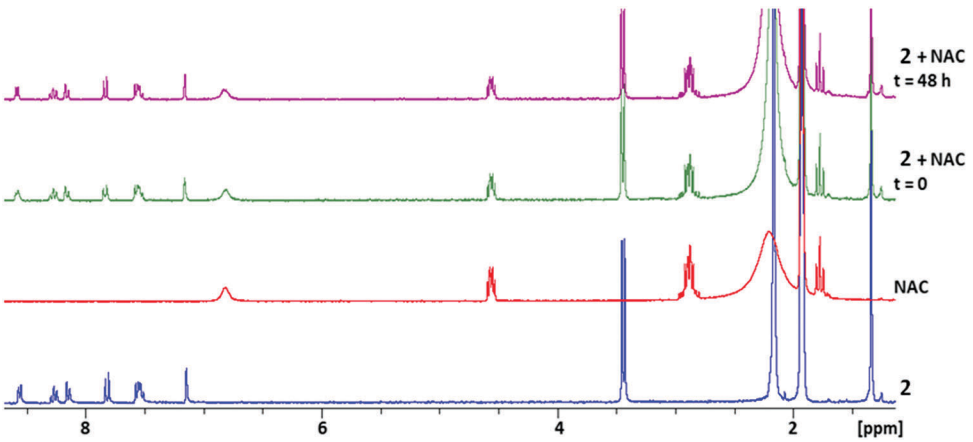

Fig. 5 ^{1}H NMR spectra of a 1 : 1 mixture of **2** with NAC at different reaction times at room temperature, in comparison with the starting materials **2** and NAC (CD_3CN).

with a (C^C) ligand. MCF-7 cells were incubated for 6 h with 10 μM concentrations of each of the complexes in 1% DMSO. The results of three independent experiments are depicted in Fig. 6.

As we previously observed for other organometallic complexes including cyclometallated Au(III) complexes,[26,27] there was a correlation between the trends in the cellular uptake study (uptake of **2** ≫ **5** > **7** > **6**) and in the *in vitro* cytotoxicity

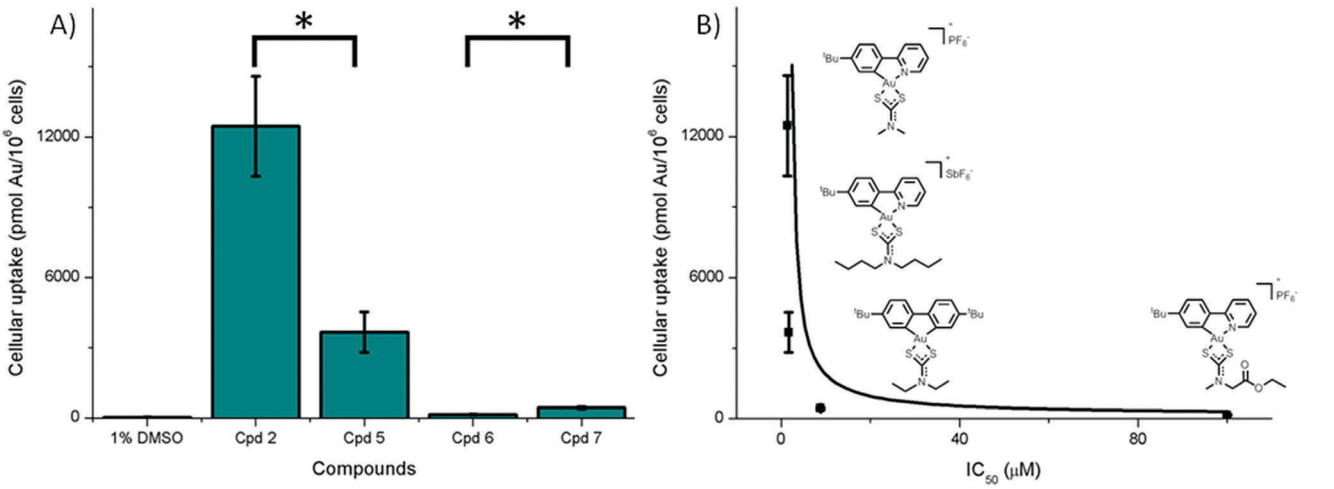

Fig. 6 (A) Cellular uptake of complexes **2**, **5**, **6** and **7** and a DMSO control in MCF-7 cells after 6 h of treatment at 10 μM in 1% DMSO. Data represent the average ± standard deviation of three experiments. The significance of the results was analysed by *t*-test. *p value < 0.05. (B) Correlation between IC_{50} and cell uptake of complexes **2**, **5**, **6** and **7** in MCF-7 cells.

study of the complexes (IC_{50} **2** ≈ **5** < **7** ≪ **6**) as depicted in Fig. 6B. The most cytotoxic complexes **2** and **5**, which have IC_{50} values of 1.4 and 1.7 μM respectively, both show high levels of uptake, particularly the dimethyl variant, **2** which displays more than three times the cellular uptake of complex **5**. Complex **7**, the neutral (C^C) dithiocarbamate, is moderately cytotoxic towards MCF-7 cells with an IC_{50} of 8.8 μM and also displays quite a low cellular uptake. Both **2** and **5** present significantly higher levels of cellular uptake than **7** (28 and 8 times respectively). Complex **6**, the most hydrophilic complex bearing a sarcosine ethyl ester substituent, has both very low *in vitro* cytotoxicity (IC_{50} value of >100 μM) and also poor cellular uptake. It seems therefore that there is a delicate balance between lipophilicity, charge and solubility under physiological conditions which must be met for compounds to be able to cross the phospholipid bilayer cell membrane. This behaviour is consistent with our previous observations on the cytotoxicity of pincer-stabilised complexes of the type $[(C^N^{pz}^C)Au(NHC)]^+$ (NHC = N-heterocyclic carbene).[27]

Quantification of reactive oxygen species

Induction of reactive oxygen species (ROS) is a recognized mechanism of action for metal-based drugs, including Au^{III}(DTC) complexes.[18b] The cyclometallated dithiocarbamate complexes investigated here were therefore tested for the production of ROS. The amount of intracellular ROS was measured after treatment of MCF-7 cells with 100 μM, 50 μM and 10 μM concentrations of each complex. The results are summarized in Fig. 7. Contrary to what has been observed in the case of $AuCl_2(S_2CNMe_2)$,[18b] none of the tested complexes appeared to increase the production of ROS and therefore this mode of action can be ruled out for these cyclometallated gold dithiocarbamates. However, this is in line with reports for other cyclometallated Au(III) complexes,[28,38] suggesting that in our case of mixed cyclometallated/DTC complexes, the inability to generate ROS is related to the cyclometallated ligand structure.

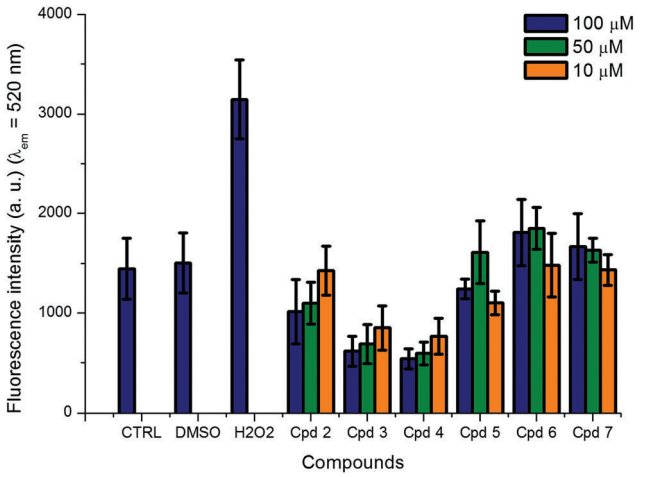

Fig. 7 ROS measurements in MCF-7 cells after 24 h incubation with complexes **2–7**.

Interactions with non-canonical DNA structures

Higher-order DNA structures like G-quadruplexes and i-motifs are emerging as promising targets for the development of new anticancer agents.[39] G-quadruplexes are four-stranded DNA secondary structures that form in guanine-rich DNA sequences. They are formed by the stacking of tetrads of guanine residues linked *via* hydrogen-bonding and stabilized by the presence of typically monovalent cations in the centre of the tetrad.[40] The selective stabilization of G-quadruplex structures has been investigated as a method of controlling key cellular events such as telomerase activity or oncogene expression making them potentially interesting anticancer targets.[39a,b] Recently, there have been several examples of potential chemotherapeutic gold(I, III) complexes that target G-quadruplexes.[27,41] A caffeine-based $[Au(NHC)_2]^+$ cation has been co-crystallized with a G-quadruplex, showing that DNA–ligand interaction occurred *via* π-stacking on the accessible tetrads.[42]

i-Motifs are higher-order DNA structures that form in cytosine-rich DNA sequences *via* hydrogen bonding between hemiprotonated pairs of cytosines. As i-motifs require cytosine-rich sequences, they are likely to form in the complementary strands opposing G-quadruplexes in the genome.[39c,d] Stabilization of i-motif structures has been shown to alter gene expression of the oncogene bcl-2 and disrupt telomerase activity, and therefore compounds that stabilize these structures also have potential as anticancer drugs.[39d]

Cyclometallated Au(III) complexes have been reported to selectively stabilize the non-canonical DNA G-quadruplex and i-motif structures.[27,41b] We thus investigated the influence of the DTC ligands on the interaction between the cyclometallated Au(III) moiety and G-quadruplexes and i-motifs.

The established Förster resonance energy transfer (FRET) based DNA melting method measures the changes in fluorescence as the spatial distance between two fluorophores at the ends of DNA is changed as they are brought closer together or moved further apart. Comparison of the melting temperature of DNA in the absence and presence of compounds can reveal any compound-induced DNA stabilization or denaturation.[43] Here, FRET results are expressed as the changes in DNA melting temperature (ΔT_m) when DNA (0.2 μM) is dosed with 50 μM concentrations of each drug. Thus the higher ΔT_m is in the presence of a compound, the higher is the DNA stabilization and thus the stronger is the compound–DNA interaction. The DNA melting assay was used to give a broad indication of the DNA binding capabilities of the dithiocarbamate complexes **2–7** towards different DNA targets. We used a G-quadruplex forming sequence from the human telomere (hTeloG), the human telomeric i-motif sequence (hTeloC), and i-motif forming sequences from the promoter regions of HIF-1-α (hif-1-α) and c-Myc (c-MycC), as well as double-stranded DNA.

The human telomeric i-motif forming sequence, hTeloC is most stable at acidic pH. The binding capabilities of the complexes were therefore assessed at a transitional pH of 6.0 (the pH where the structure is 50% folded).[44] The c-MYC i-motif, is also more stable at acidic pH, was measured at the respective transitional pH of 6.6.[39d] The remaining sequences were all tested at the transitional pH of hif-1-α, pH 7.2.[45] Results of the FRET-melting assay with complexes **2–7** are depicted in Fig. 8.

Complexes **2**, **3**, **4** and **5** showed high levels of DNA stabilization towards all higher-order DNA structures tested. These four complexes showed particularly high levels of stabilization towards two of the i-motif forming sequences, the human telomeric i-motif sequence, (hTeloC) and the i-motif forming sequence from the promoter region of c-Myc (c-MycC). For these two sequences, ΔT_m values were between 47–51 °C for complexes **2**, **3** and **4** and >60 °C for complex **5**. For the G-quadruplex forming sequence, (hTeloG) and the i-motif forming sequence, (hif-1-α), ΔT_m values were somewhat lower, between 26–37 °C for all four complexes, indicating lower levels of complex–DNA stabilization and thus weaker DNA binding.

In good agreement with the cytotoxicity data, both **6**, the least cytotoxic of the $[(C^N)Au(DTC)]^+$ complexes, and **7**, the neutral (C^C)Au(DTC), showed only low levels of DNA interaction towards all tested structures. For both types of complexes, ΔT_m values were below 10 °C for all of the DNA structures tested. These values could be a result of the lack of a cationic charge as this is consistent with our previous work, which highlights the importance of a cationic charge on the ability of gold complexes to interact with higher-order nucleic acid structures.[27] This suggests that mixed cyclometallated/dithiocarbamate Au(III) complexes behave similarly to pure cyclometallated Au(III) complexes, with the nature of the DTC ligand acting only to modulate the strength of the gold complex/DNA interaction. The results of the FRET-melting assay are generally in good agreement with the cytotoxicity data, with the most cytotoxic complexes displaying the highest levels of stabilization of the higher-order DNA structures. This suggests that the stabilization of these structures could be a possible mechanism of action of these complexes.

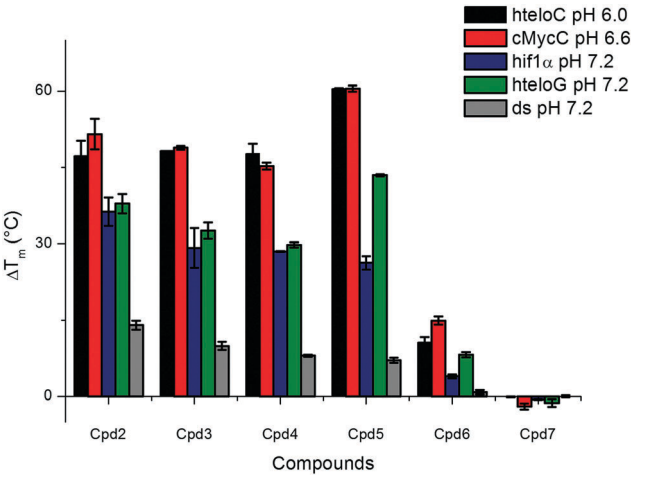

Fig. 8 Stabilization of different DNA structures (0.2 μM) in 10 mM sodium cacodylate, 100 mM NaCl when dosed with 50 μM concentrations of dithiocarbamate complexes **2–7**. Data represents the average and standard deviations of two experiments.

Inhibition of thioredoxin reductase

Thioredoxin reductase (TrxR) is a homodimeric enzyme whose role consists of reducing thioredoxin (Trx) in an NADPH-dependent manner. Trx is responsible for the subsequent reduction of different proteins including ribonucleotide reductase and peroxiredoxin. Such inhibition of TrxR leads to apoptosis through mitochondrial membrane permeabilization and release of cytochrome *c*.[46] Gold complexes are well-known to selectively inhibit TrxR over the closely related enzyme glutathione reductase *via* the direct coordination of the gold cation to the selenocysteine residue present in the active site of TrxR.[47] Considering that dithiocarbamate Au(III) complexes[18b] and, in some cases depending on the ancillary ligand, cyclometallated Au(III) complexes[15] have been reported to inhibit TrxR, and taking into account the ability of our $[(C^N)Au(DTC)]^+$ complexes to react with the thiol containing tripeptide GSH, we tested complex **3**, as a representative of that class of compounds,

in vitro as a potential TrxR inhibitor using mammalian TrxR (see Experimental part for details). The IC_{50} of complex **3** was 0.31 ± 0.03 μM, demonstrating TrxR as another potential intracellular target of that class of compounds. It is worth noting that this value is intermediate between those of pure cyclometallated complexes (tenth to low micromolar range)[15] and those of pure dithiocarbamate complexes (low nanomolar range).[18b] This suggests the possibility to modulate the inhibitory activity of Au(III) complexes through the association of cyclometallated and dithiocarbamate ligands.

Conclusions

Cyclometallated gold(III) dithiocarbamate complexes of the type $[(C\hat{}N)Au^{III}(S_2CNR_2)]^+$ show cytotoxicities that vary with the length and polarity of the *N*-alkyl substituents R and decrease in the order R = Me ≈ Et > pyrrolidine ≈ ^{n}Bu ≫ sarcosine ethyl ester, with cationic complexes being much more active than neutral (C^C)-chelated analogues. The complexes were tested for their *in vitro* cytotoxicity towards a panel of human cancer cell lines including lung adenocarcinoma cells (A549), breast adenocarcinoma (MCF-7 and MDA-MB-231), human colon cancer (HCT-116) and promyelocytic leukaemia (HL60), as well as healthy Human Umbilical Vein Endothelial Cells (HUVEC) for comparison. Complexes **2**, **3**, **4** and **5** showed the highest levels of cytotoxicity with IC_{50} values dropping to sub-micromolar levels. The most hydrophilic complex, **6**, the sarcosine ethyl ester derivative, was non-toxic across all of the cell lines. The most lipophilic complex, the (C^C) derivative **7**, also showed only low cytotoxicity. Cellular uptake studies in MCF-7 breast cancer cells indicated that there was a correlation between the *in vitro* cytotoxicity of the complexes and their ability to enter the cell. Complex **2** and **5** both showed high levels of cellular uptake in comparison to **6** and **7**. However, this correlation is non-linear, and therefore cell uptake is only one of the preconditions for cytotoxicity.

Redox stability and mechanistic studies on targets have been carried out, including ROS production for the (DTC)Au(III) complexes and G-quadruplex and i-motif DNA structures for the cyclometallated Au(III) compounds, as well as TrxR inhibition studies as a common target to both classes of compounds. This has enabled us to investigate the influence of each structural element on the pharmacological properties of the other. We observed that cyclometallated gold(III) dithiocarbamate complexes presented an intermediate redox stability between the pure cyclometallated and pure dithiocarbamate Au(III) complexes. The presence of a cyclometallated ligand completely inhibited the ability of the (DTC)Au(III) to generate ROS, while the interaction of the mixed complexes with G-quadruplexes and i-motifs followed the same trend as for non-DTC cyclometallated Au(III), with only a small influence of the nature of the DTC ligand. Moreover, complex **3** presented an intermediate inhibitory activity against TrxR between those of the pure cyclometallated and dithiocarbamate Au(III) complexes, suggesting that cyclometallated/dithiocarbamate Au(III) complexes should be considered as an independent class of compounds in some cases. Altogether these data highlight the potential of fine tuning the reactivity of this class of organogold complexes.

For a better understanding of the full mechanism of action, the activity of cyclometallated/dithiocarbamate Au(III) complexes against other reported targets of each single classes, such as proteasome, PARP-1 or cathepsins, should be investigated. Moreover, beyond those reported targets, specific targets of this peculiar class of compound might emerge.

Experimental

When required, manipulations were performed using standard Schlenk techniques under dry nitrogen or in an MBraun glove box. Nitrogen was purified by passing through columns of supported P_2O_5 with moisture indicator, and activated 4 Å molecular sieves. Anhydrous solvents were freshly distilled from appropriate drying agents. ^{1}H and $^{13}C\{^1H\}$ spectra were recorded using a Bruker Avance DPX-300 spectrometer. ^{1}H NMR spectra (300.13 MHz) were referenced to the residual protons of the deuterated solvent used. $^{13}C\{^1H\}$ NMR spectra (75.47 MHz) were referenced internally to the D-coupled ^{13}C resonances of the NMR solvent. Elemental analyses were carried out at London Metropolitan University. $(C\hat{}N)AuCl_2$ (**1**) and compound **7** were synthesized following reported procedures [C^N = 2-(4′-*t*-butylphenyl-2′-yl)pyridine].[23,24]

Synthesis of complex 2

A solution of sodium dimethyldithiocarbamate hydrate (0.020 g, 0.140 mmol) in methanol (10 mL) was added dropwise to a suspension of $(C\hat{}N)AuCl_2$ (0.060 g, 0.125 mmol) in methanol (15 mL) and stirred at room temperature overnight. A colour change from white to pale yellow was observed during the addition. An excess of a saturated aqueous solution of KPF_6 was then added, which caused an immediate fluffy white precipitation. The solid was filtered off and purified by dissolving in a minimal amount of acetonitrile (2 mL) and precipitating with excess diethyl ether (20 mL). The product was filtered and dried under vacuum (0.069 g, 0.103 mmol, 82%). Anal. calcd for $C_{18}H_{22}AuF_6N_2PS_2{\cdot}5H_2O$ (762.51): C, 28.35; H, 4.23; N, 3.67. Found C, 28.15; H, 3.98; N, 3.69. ^{1}H NMR ($(CD_3)_2SO$, 300 MHz, 298 K): δ 8.74 (d, $^3J_{H-H}$ = 6.0 Hz, 1H, H^2), 8.43–8.30 (m, 2H, H^{4+5}), 7.99 (d, $^3J_{H-H}$ = 8.2 Hz, 1H, H^8), 7.60 (t, $^3J_{H-H}$ = 6.0 Hz, 1H, H^3), 7.53 (d, $^3J_{H-H}$ = 8.2 Hz, 1H, H^9), 7.03 (s, 1H, H^{11}), 3.49 (s, 3H, $H^{14/14'}$), 3.44 (s, 3H, $H^{14/14'}$), 1.28 (s, 9H, ^{t}Bu). $^{13}C\{^1H\}$ NMR ($(CD_3)_2SO$, 75 MHz): δ 193.3 (s, C^{13}), 163.7 (s, C^{12}), 155.8 (s, $C^{6/7}$), 151.6 (s, $C^{6/7}$), 150.1 (s, C^2), 144.1 (s, C^4), 141.8 (s, C^{10}), 127.5 (s, C^8), 126.7 (s, C^9), 126.2 (s, C^3), 124.7 (s, C^{11}), 122.6 (s, C^5), 42.5 (s, C^{14}), 41.2 (s, $C^{14'}$), 35.9 (s, $C(CH_3)_3$), 31.2 (s, $C(CH_3)_3$). IR: ν_{max}(neat)/cm^{-1}: 1579 (dithiocarbamate).

Synthesis of complex 3

Following the procedure described for **2**, complex **3** was made from $(C\hat{}N)AuCl_2$ (0.060 g, 0.125 mmol) and $NaS_2CNEt_2{\cdot}H_2O$ (0.028 g, 0.125 mmol) as a white microcrystalline solid

(0.083 g, 0.118 mmol, 94%). Anal. calcd for $C_{20}H_{26}AuF_6N_2PS_2{\cdot}6H_2O$ (808.58): C, 29.71; H, 4.74; N, 3.46. Found C, 29.46; H, 4.52; N, 3.55. ^{1}H NMR ($(CD_3)_2SO$, 300 MHz, 298 K): δ 8.78 (d, $^3J_{H-H}$ = 5.4 Hz, 1H, H^2), 8.45–8.31 (m, 2H, H^{4+5}), 8.00 (d, $^3J_{H-H}$ = 8.2 Hz, 1H, H^8), 7.60 (t, $^3J_{H-H}$ = 5.4 Hz, 1H, H^3), 7.54 (dd, $^3J_{H-H}$ = 8.2 Hz, $^4J_{H-H}$ = 1.2 Hz, 1H, H^9), 7.06 (d, $^4J_{H-H}$ = 1.2 Hz, 1H, H^{11}), 3.87 (m, 4H, $H^{14+14'}$), 1.35 (m, 6H, $H^{15+15'}$), 1.29 (s, 9H, ^{t}Bu). $^{13}C\{^1H\}$ NMR ($(CD_3)_2SO$, 75 MHz): δ 193.3 (s, C^{13}), 163.6 (s, C^{12}), 155.9 (s, $C^{6/7}$), 151.7 (s, $C^{6/7}$), 150.1 (s, C^2), 144.2 (s, C^4), 141.8 (s, C^{10}), 127.5 (s, C^8), 126.6 (s, C^9), 126.1 (s, C^3), 124.8 (s, C^{11}), 122.6 (s, C^5), 48.8 (s, C^{14}), 47.3 (s, $C^{14'}$), 35.9 (s, $C(CH_3)_3$), 31.2 (s, $C(CH_3)_3$), 13.0 (s, C^{15}), 12.5 (s, $C^{15'}$). IR: ν_{max} (neat)/cm^{-1}: 1559.

Synthesis of complex 4

Following the procedure described for **2**, complex **4** was made from (C^N)$AuCl_2$ (0.060 g, 0.125 mmol) and sodium pyrrolidinedithiocarbamate hydrate (0.085 g, 0.502 mmol). A colour change from white to pale yellow was observed during the addition. This solid product was filtered and dried under vacuum (0.062 g, 0.089 mmol, 71%). Anal. calcd for $C_{20}H_{24}AuF_6N_2PS_2{\cdot}4H_2O$ (770.54): C, 31.18; H, 4.19; N, 3.64. Found C, 30.85; H, 3.78; N, 3.25. ^{1}H NMR (CD_2Cl_2, 300 MHz, 298 K): δ 8.48 (d, $^3J_{H-H}$ = 5.6 Hz, 1H, H^2), 8.26 (dt, $^3J_{H-H}$ = 8.1 Hz, $^4J_{H-H}$ = 1.5 Hz, 1H, H^4), 8.07 (d, $^3J_{H-H}$ = 8.1 Hz, 1H, H^5), 7.72 (d, $^3J_{H-H}$ = 8.3 Hz, 1H, H^8), 7.59–7.50 (m, 2H, H^{3+9}), 7.13 (d, $^4J_{H-H}$ = 1.6 Hz, 1H, H^{11}), 3.98 (t, $^3J_{H-H}$ = 6.6 Hz, 4H, $H^{14+14'}$), 2.24 (m, 4H, $H^{15+15'}$), 1.36 (s, 9H, ^{t}Bu). $^{13}C\{^1H\}$ NMR (CD_2Cl_2, 75 MHz): δ 190.4 (s, C^{13}), 164.4 (s, C^{12}), 157.1 (s, $C^{6/7}$), 151.8 (s, $C^{6/7}$), 148.4 (s, C^2), 143.6 (s, C^4), 140.5 (s, C^{10}), 126.6 (s, C^8), 126.5 (s, C^9), 125.3 (s, C^3), 125.3 (s, C^{11}), 122.0 (s, C^5), 52.0 (s, $C^{14/14'}$), 35.8 (s, $C(CH_3)_3$), 30.7 (s, $C(CH_3)_3$), 24.6 (s, $C^{15/15'}$), 24.2 (s, $C^{15/15'}$). IR: ν_{max} (neat)/cm^{-1}: 1556.

Synthesis of complex 5

Following the procedure described for **2**, complex **5** was made from (C^N)$AuCl_2$ (0.060 g, 0.125 mmol) and $NaS_2CN^nBu_2$ (0.105 g, 0.379 mmol). A colour change from white to pale yellow was observed during the addition. The solvent was removed under vacuum and the dark yellow residue was dissolved in dichloromethane (15 mL). Excess $AgSbF_6$ in dichloromethane (5 mL) was then added and the solvent was removed under vacuum. The solid was purified by dissolving in minimal acetonitrile (2 mL) and precipitating the product with an excess of diethyl ether (20 mL). This was filtered and dried under vacuum (0.073 g, 0.086 mmol, 71%). Anal. calcd for $C_{24}H_{34}AuF_6N_2S_2Sb{\cdot}2MeCN$ (929.49): C, 36.18; H, 4.34; N, 6.03. Found C, 35.70; H, 3.96; N, 6.09. ^{1}H NMR (CD_3CN, 300 MHz, 298 K): δ 8.40 (d, $^3J_{H-H}$ = 5.6 Hz, 1H, H^2), 8.23 (dt, $^3J_{H-H}$ = 8.1 Hz, $^4J_{H-H}$ = 1.4 Hz, 1H, H^4), 8.06 (d, $^3J_{H-H}$ = 8.1 Hz, 1H, H^5), 7.71 (d, $^3J_{H-H}$ = 8.1 Hz, 1H, H^8), 7.55–7.44 (m, 2H, H^{3+9}), 7.08 (d, $^4J_{H-H}$ = 1.7 Hz, 1H, H^{11}), 3.77 (m, 4H, $H^{14+14'}$), 1.78 (m, 4H, $H^{15+15'}$), 1.42 (m, 4H, $H^{16+16'}$), 1.33 (s, 9H, ^{t}Bu), 0.98 (m, 6H, $H^{17+17'}$). $^{13}C\{H\}$ NMR (CD_3CN, 75 MHz): δ 194.4 (s, C^{13}), 163.8 (s, C^{12}), 156.4 (s, $C^{6/7}$), 151.6 (s, $C^{6/7}$), 148.9 (s, C^2), 143.6 (s, C^4), 141.1 (s, C^{10}), 126.7 (s, C^8), 126.5 (s, C^9), 125.5 (s, C^3), 125.0 (s, C^{11}), 122.1 (s, C^5), 53.6 (s, $C^{14/14'}$), 52.0 (s, $C^{14/14'}$), 35.5 (s, $C(CH_3)_3$), 30.2 (s, $C(CH_3)_3$), 28.9 (s, $C^{15/15'}$), 28.6 (s, $C^{15/15'}$), 19.6 (s, $C^{16/16'}$), 12.9 (s, $C^{17/17'}$). IR: ν_{max} (neat)/cm^{-1}: 1550.

Synthesis of complex 6

Following the procedure described for **2**, complex **6** was made from (C^N)$AuCl_2$ (0.060 g, 0.125 mmol) and sarcosine ethyl ester dithiocarbamate hydrate (0.100 g, 0517 mmol). The solid was filtered and purified by dissolving in minimal acetonitrile (2 mL) and precipitating the product with an excess of diethyl ether (20 mL). The product was filtered and dried under vacuum (0.073 g, 0.098 mmol, 78%). Anal. calcd for $C_{21}H_{26}AuF_6N_2PS_2{\cdot}8H_2O$ (906.64): C, 27.82; H, 4.89; N, 3.09. Found C, 27.34; H, 4.42; N, 3.29. ^{1}H NMR ($(CD_3)_2SO$, 300 MHz, 298 K): δ 8.77 (d, $^3J_{H-H}$ = 5.6 Hz, 0.8H, $H^{2'}$), 8.71 (d, $^3J_{H-H}$ = 5.6 Hz, 1H, H^2), 8.40–8.27 (m, 3.6H, $H^{4+4'+5+5'}$), 7.94 (m, 1.8H, $H^{9+9'}$), 7.63–7.49 (m, 3.6H, $H^{3+3'+8+8'}$), 7.15 (d, $^4J_{H-H}$ = 1.4 Hz, 1H, H^{11}), 7.01 (d, $^4J_{H-H}$ = 1.4 Hz, 0.8H, $H^{11'}$), 4.82 (s, 1.6H, $H^{15'}$), 4.78 (s, 2H, H^{15}), 4.21 (m, 3.6H, $H^{17+17'}$), 3.54 (s, 3H, H^{14}), 3.45 (s, 2.4H, $H^{14'}$), 1.29 (s, 9H, ^{t}Bu), 1.27 (s, 7.2H, ^{t}Bu′), 1.23 (m, 5.4H, $H^{18+18'}$). $^{13}C\{^1H\}$ NMR ($(CD_3)_2SO$, 75 MHz): δ 198.7 (s, C^{13}), 166.3 (s, $C^{16'}$), 166.2 (s, C^{16}), 163.5 (s, $C^{12'}$), 163.3 (s, C^{12}), 156.0 (s, $C^{6'/7'}$), 156.0 (s, $C^{6/7}$), 151.5 (s, $C^{6'/7'}$), 151.2 (s, $C^{6/7}$), 150.1 (s, $C^{2'}$), 150.0 (s, C^2), 144.1 (s, $C^{4'}$), 144.1 (s, C^4), 141.6 (s, $C^{10'}$), 141.4 (s, C^{10}), 127.4 (s, $C^{8'}$), 127.4 (s, C^8), 126.8 (s, $C^{9'}$), 126.7 (s, C^9), 126.1 (s, C^3), 126.0 (s, $C^{3'}$), 124.7 (s, $C^{11'}$), 124.7 (s, C^{11}), 122.5 (s, $C^{5'}$), 122.5 (s, C^5), 62.6 (s, $C^{14'}$), 62.6 (s, C^{14}), 55.3 (s, $C^{15'}$), 54.1 (s, C^{15}), 35.9 (s, $C(CH_3)_3$), 31.4 (s, $C^{17'}$), 31.1 (s, $C(CH_3)_3$), 30.0 (s, C^{17}), 14.3 (s, C^{18}), 14.3 (s, $C^{18'}$). IR: ν_{max} (neat)/cm^{-1}: 1736 (C═O), 1558 (dithiocarbamate).

X-Ray diffraction

Crystal data. $2(C_{20}H_{26}AuN_2S_2)$, $2(PF_6)$, MeCN, M = 1442.02; CCDC code: 1854835.† Monoclinic, space group $P2_1/c$ (no. 14), a = 11.9382(2), b = 26.6092(3), c = 16.1416(3) Å, β = 93.060(2)°, V = 5120.33(14) Å^3. Z = 4, D_c = 1.871 g cm^{-3}, $F(000)$ = 2808, T = 140(1) K, μ(Mo-Kα) = 60.3 cm^{-1}, λ(Mo-Kα) = 0.71073 Å.

Crystals are large, pale yellow-green prisms. From a sample under oil, one, a block (fragment) *ca.* 0.10 × 0.21 × 0.33 mm, was mounted on a glass fibre and fixed in a cold nitrogen stream on an Oxford Diffraction Xcalibur-3/Sapphire3-CCD diffractometer equipped with Mo-Kα radiation and graphite monochromator. Intensity data were measured by thin-slice ω- and φ-scans. Total no. of reflections recorded, to θ_{max} = 27.5°, was 87 240 of which 11 737 were unique (R_{int} = 0.036); 10 802 were 'observed' with $I > 2\sigma_I$.

Data were processed using the CrysAlisPro-CCD and -RED[48] programs. The structure was determined by the intrinsic phasing routines in the SHELXT program[49] and refined by full-matrix least-squares methods, on F^2's, in SHELXL.[50] The non-hydrogen atoms were refined with anisotropic thermal parameters. Hydrogen atoms were included in idealised positions and their U_{iso} values were set to ride on the U_{eq} values of the parent carbon atoms. At the conclusion of the refinement, wR_2 = 0.049 and R_1 = 0.029 (47) for all 11 737 reflections weighted w = $[\sigma^2(F_o^2) + (0.0117P)^2 + 10.284P]^{-1}$ with $P = (F_o^2 + 2F_c^2)/3$; for the 'observed' data only, R_1 = 0.024.

In the final difference map, the highest peaks (to *ca.* 1.0 e Å^{-3}) were close to the gold atoms.

Scattering factors for neutral atoms were taken from ref. 51. Computer programs used in this analysis have been noted above,

and were run through WinGX[52] on a Dell Precision 370 PC at the University of East Anglia.

Antiproliferation assay

The human A549 and HL60 cancer cell lines (from ECACC) were cultured in RPMI 1640 medium with 10% fetal calf serum, 2 mM L-glutamine, 100 U mL^{-1} penicillin and 100 μg mL^{-1} streptomycin (Invitrogen). The cells were maintained under a humidified atmosphere at 37 °C and 5% CO_2. The human MCF-7, HCT116 and MDA-MB-231 cancer cell lines (from ECACC) were cultured in DMEM medium with 10% fetal calf serum, 2 mM L-glutamine, 100 U mL^{-1} penicillin and 100 μg mL^{-1} streptomycin (Invitrogen). The HUVEC cells were cultured in Endothelial Cell Growth Medium with growth and antibiotic supplement. The cells were maintained under a humidified atmosphere at 37 °C and 5% CO_2. Inhibition of cancer cell proliferation was measured by the 3-(4,5-dimethylthiazol-2-yl)5-(3-carboxymethoxyphenyl)-2-(4-sulfophenyl)-2*H*-tetrazolium (MTS) assay using the CellTiter 96 Aqueous One Solution Cell Proliferation Assay (Promega) and following the manufacturer's instructions. Briefly, the cells (3×10^4 per 100 μL for HL60, 8×10^3 per 100 μL for A549, MCF-7, HCT116, MDA-MB-231 and HUVEC) were seeded in 96-well plates and left untreated or treated with 1 μL of DMSO (vehicle control) or 1 μL of complexes diluted in DMSO at different concentrations, in triplicate for 72 h at 37 °C with 5% CO_2. Following this, MTS assay reagent was added for 4 h and absorbance measured at 490 nm using a Polarstar Optima microplate reader (BMG Labtech). IC_{50} values were calculated using GraphPad Prism Version 5.0 software.

Uptake study

MCF-7 cells were grown in 75 cm^2 flasks up to 70% of confluence in 10 mL of culture medium. Compounds **2**, **5**, **6** and **7** were added to the flasks (100 μL of 1 mM solution in DMSO) and incubated for 6 h at 37 °C with 5% CO_2. Negative controls were used by incubating cells with DMSO alone under the same conditions. After removal of the medium and washing of the cells with PBS pH 7.4, the cells were detached using a trypsin solution. After quenching of trypsin with fresh medium, centrifugation and removal of the supernatant, the cell pellet was resuspended into 1 mL of PBS pH 7.4 and split into twice 500 μL for metal and protein quantification. The number of cells (expressed per million cells) of each sample was determined by measuring the protein content of the treated samples using a BCA assay (ThermoFischer Scientific) corrected by the amount of protein/10^6 cells determined for each cell type by measuring the protein content of an untreated sample and dividing by the corresponding number of cells measured with a hematocytometer following a reported procedure.[53] Microwave digestion was used to solvate the samples to liquid form. Nitric acid and hydrogen peroxide were used in a Milestone Ethos 1 microwave system using SK-10 10 place carousel. The digest was ramped to 200 °C in 15 min, holding at 200 °C for 15 min. The sample was weighed into a microwave vessel before digestion, and decanted and rinsed into a pre-weighed PFA bottle after digestion. ICP-MS samples were spiked with rhodium internal standard and run on a Thermo X series 1 ICP-MS. The isotopes selected were ^{63}Cu, ^{65}Cu, ^{107}Ag, ^{109}Ag and ^{197}Au. Certified standards and independent reference were used for accuracy. Acid blanks were run through the system and subtracted from sample measurements before corrections for dilution.

ROS assay

100 μL of MCF-7 cells were seeded at a density of 1×10^5 cells per mL in a 96-well black plate with a transparent bottom. The cells were incubated at 37 °C for 24 h. The medium was removed, and replaced with 50 μM H_2DCFDA (from Life Technologies) solution in PBS for 40 min. H_2DCFDA was removed and replaced with fresh medium. The cells were left for recovery for 20 min at 37 °C. Basal fluorescence was measured at 485/520 nm on a POLARstar Optima. The cells were incubated with 10 μM, 50 μM, or 100 μM of compounds, 1% DMSO (negative control) and 100 μM of H_2O_2 (positive control) for 24 h. Fluorescence was read at 485/520 nm. Basal fluorescence was subtracted from the fluorescence in the treated cells to calculate the amount of fluorescence caused by the compounds.

FRET melting assay

Assessment of compound-induced stabilization of DNA was performed using a fluorescence resonance energy transfer (FRET) DNA melting based assay. The sequences used were hTeloC$_{FRET}$ (5′-FAM-d[TAA-CCC-TAA-CCC-TAA-CCC-TAA-CCC]-TAMRA-3′); hif-1-α$_{FRET}$ (5′-d[CGC-GCT-CCC-GCC-CCC-TCT-CCC-CTC-CCC-GCG-C]-TAMRA-3′), hTeloG$_{FRET}$ (5′-FAM-d[GGG-TTA-GGG-TTA-GGG-TTA-GGG]-TAMRA-3′), cMycC$_{FRET}$ (5′-FAM-d-[CCC-CAC-CTT-CCC-CAC-CCT-CCC-CAC-CCT-CCC-C]-TAMRA-3′) and DS$_{FRET}$ (FAM-d(TAT-AGC-TAT-A-HEG(18)-TAT-AGC-TAT-A)-TAMRA-3′). The labelled oligonucleotides (donor fluorophore FAM is 6-carboxyfluorescein; acceptor fluorophore TAMRA is 6-carboxytetramethyl-rhodamine) were prepared as a 220 nM solution in 10 mM sodium cacodylate buffer at the indicated pH with 100 mM sodium chloride and then thermally annealed by heating to 95 °C in a heat block and cooling overnight. Striptubes (QIAgen) were prepared by aliquoting 20 μL of the annealed DNA, followed by 0.5 μL of the compound solutions. Control samples for each run were prepared with the same quantity of DMSO with the DNA in buffer. Fluorescence melting curves were determined in a QIAgen Rotor-Gene Q-series PCR machine, using a total reaction volume of 20 μL. Measurements were made with excitation at 470 nm and detection at 510 nm. Final analysis of the data was carried out using QIAgen Rotor-Gene Q-series software and Origin or Excel.

Inhibition of mammalian TrxR

To determine the inhibition of mammalian TrxR, an established microplate-reader-based assay was performed.[54] For this purpose, commercially available rat liver TrxR (Sigma Aldrich) was used and diluted with distilled water to achieve a concentration of 3.58 U mL^{-1}. The compound was freshly dissolved as stock solutions in DMSO. Aliquots (25 mL) of the enzyme

solution and either potassium phosphate buffer (25 μL; pH 7.0) containing the compound in graded concentrations or buffer (25 μL) without the compound, but DMSO (positive control) were added. A blank solution (DMSO in buffer; 50 μL) was also prepared (final concentrations of DMSO: 0.5% v/v). The resulting solutions were incubated with moderate shaking for 75 min at 37 °C in a 96-well plate. A portion (225 μL) of the reaction mixture (1 mL of reaction mixture consists of: 500 μL potassium phosphate buffer pH 7.0, 80 μL EDTA solution (100 mM, pH 7.5), 20 μL BSA solution (0.2%), 100 μL of NADPH solution (20 mM), and 300 μL distilled water) was added to each well and the reaction was immediately initiated by the addition of 20 mM DTNB solution in ethanol (25 μL). After thorough mixing, the formation of 5-TNB was monitored with a microplate reader at 405 nm ten times in 35 second intervals for about 6 min. The increase in 5-TNB concentration over time followed a linear trend (r^2 = 0.990), and the enzymatic activities were calculated as the slopes thereof (increase in absorbance per second). For each tested compound, the non-interference with the assay components was confirmed by a negative control experiment using an enzyme-free test solution. IC_{50} values were calculated as the concentration of the compounds decreasing the enzymatic activity of the untreated control by 50%, and are given as the means and error of three repeated experiments.

Conflicts of interest

There are no conflicts of interest to declare.

Acknowledgements

This work was supported by the European Research Council. M. B. is an ERC Advanced Investigator Award holder (grant no. 338944-GOCAT).

References

1 (*a*) B. Rosenberg, L. Vancamp and T. Krigas, *Nature*, 1965, **205**, 698–699; (*b*) B. Rosenberg, L. Van Camp, J. E. Trosko and V. H. Mansour, *Nature*, 1969, **222**, 385–386.
2 R. Oun, Y. E. Moussa and N. J. Wheate, *Dalton Trans.*, 2018, **47**, 6645–6653.
3 G. Jaouen, A. Vessières and S. Top, *Chem. Soc. Rev.*, 2015, **44**, 8802–8817.
4 C. Santini, M. Pellei, V. Gandin, M. Porchia, F. Tisato and C. Marzano, *Chem. Rev.*, 2013, **114**, 815–862.
5 G. Süss-Fink, *Dalton Trans.*, 2010, **39**, 1673–1688.
6 (*a*) I. Ott, *Coord. Chem. Rev.*, 2009, **253**, 1670–1681; (*b*) S. J. Berners-Price and A. Filipovska, *Metallomics*, 2011, **3**, 863–873; (*c*) T. Zou, C. T. Lum, C.-N. Lok, J.-J. Zhang and C.-M. Che, *Chem. Soc. Rev.*, 2015, **44**, 8786–8801.
7 (*a*) B. Bertrand and A. Casini, *Dalton Trans.*, 2014, **43**, 4209–4219; (*b*) L. Oehninger, R. Rubbiani and I. Ott, *Dalton Trans.*, 2013, **42**, 3269–3284; (*c*) B. Bertrand, M. R. M. Williams and M. Bochmann, *Chem. – Eur. J.*, 2018, **24**, 11840–11851.
8 (*a*) R. D. Fan, C.-T. Yang, J. D. Ranford, J. J. Vittal and P. F. Lee, *Dalton Trans.*, 2003, 3376–3381; (*b*) M. Coronnello, E. Mini, B. Caciagli, M. A. Cinellu, A. Bindoli, C. Gabbiani and L. Messori, *J. Med. Chem.*, 2005, **48**, 6761–6765; (*c*) R. W.-Y. Sun, C.-N. Lok, T. T.-H. Fong, C. K.-L. Li, Z. F. Yang, T. Zou, A. F.-M. Siu and C.-M. Che, *Chem. Sci.*, 2013, **4**, 1979–1988.
9 B. Bertrand, M. Bochmann, J. Fernandez-Cestau and L. Rocchigiani, in *Pincer Compounds – Chemistry and Applications*, ed. D. Morales-Morales, Elsevier, Amsterdam, 2018, ch. 31, pp. 673–699.
10 R. V. Parish, B. P. Howe, J. P. Wright, J. Mack, R. G. Pritchard, R. G. Buckley, A. M. Elsome and S. P. Fricker, *Inorg. Chem.*, 1996, **35**, 1659–1666.
11 Y. Zhu, B. R. Cameron, R. Mosi, V. Anastassov, J. Cox, L. Qin, Z. Santucci, M. Metz, R. T. Skerlj and S. P. Fricker, *J. Inorg. Biochem.*, 2011, **105**, 754–762.
12 D. Fan, C.-T. Yang, J. D. Ranford, P. F. Lee and J. J. Vittal, *Dalton Trans.*, 2003, 2680–2685.
13 M. Frik, J. Fernández-Gallardo, O. Gonzalo, V. Mangas-Sanjuan, M. González-Alvarez, A. S. del Valle, C. Hu, I. González-Alvarez, M. Bermejo, I. Marzo and M. Contel, *J. Med. Chem.*, 2015, **58**, 5825–5841.
14 S. Jürgens, F. E. Kühn and A. Casini, *Curr. Med. Chem.*, 2018, **25**, 437–461.
15 R. Rubbiani, T. N. Zehnder, C. Mari, O. Blacque, K. Venkatesan and G. Gasser, *ChemMedChem*, 2014, **9**, 2781–2790.
16 B. Bertrand, S. Spreckelmeyer, E. Bodio, F. Cocco, M. Picquet, P. Richard, P. Le Gendre, C. Orvig, M. A. Cinellu and A. Casini, *Dalton Trans.*, 2015, **44**, 11911–11918.
17 J. J. Zhang, R. W. Y. Sun and C.-M. Che, *Chem. Commun.*, 2012, **48**, 3388–3390.
18 (*a*) L. Ronconi, L. Giovagnini, C. Marzano, F. Bettio, R. Graziani, G. Pilloni and D. Fregona, *Inorg. Chem.*, 2005, **44**, 1867–1881; (*b*) D. Saggioro, M. P. Rigobello, L. Paloschi, A. Folda, S. A. Moggach, S. Parsons, L. Ronconi, D. Fregona and A. Bindoli, *Chem. Biol.*, 2007, **14**, 1128–1139; (*c*) L. Cattaruzza, D. Fregona, M. Mongiat, L. Ronconi, A. Fassina, A. Colombatti and D. Aldinucci, *Int. J. Cancer*, 2011, **128**, 206–215.
19 M. Altaf, M. Monim-ul-Mehboob, A.-N. Kawde, G. Corona, R. Larcher, M. Ogasawara, N. Casagrande, M. Celegato, C. Borghese, Z. H. Siddik, D. Aldinucci and A. A. Isab, *Oncotarget*, 2017, **8**, 490–505.
20 (*a*) V. Milacic, D. Chen, L. Ronconi, K. R. Landis-Piwowar, D. Fregona and Q. P. Dou, *Cancer Res.*, 2006, **66**, 10478–10486; (*b*) J. Quero, S. Cabello, T. Fuertes, I. Marmol, R. Laplaza, V. Polo, M. C. Gimeno, M. J. Rodriguez-Yoldi and E. Cerrada, *Inorg. Chem.*, 2018, **17**, 10832–10845.
21 N. Shaik, A. Martinez, I. Augustin, H. Giovinazzo, A. Varela-Ramirez, M. Sanau, R. J. Aguilera and M. Contel, *Inorg. Chem.*, 2009, **48**, 1577–1587.
22 J. J. Zhang, K. M. Ng, C. N. Lok, R. W. Y. Sun and C.-M. Che, *Chem. Commun.*, 2013, **49**, 5153–5155.
23 E. C. Constable and T. A. Leese, *J. Organomet. Chem.*, 1989, **363**, 419–424.

24 B. David, U. Monkowius, J. Rust, C. W. Lehmann, L. Hyzak and F. Mohr, *Dalton Trans.*, 2014, **43**, 11059–11066.
25 M. Altaf, A. A. Isab, J. Vanco, Z. Dvorak, Z. Travnicek and H. Stoeckli-Evans, *RSC Adv.*, 2015, **5**, 81599–81607.
26 F. Chotard, L. Dondaine, C. Balan, A. Bettaïb, C. Paul, P. Le Gendre and E. Bodio, *New J. Chem.*, 2018, **42**, 8105–8112.
27 B. Bertrand, J. Fernandez-Cestau, J. Angulo, M. M. D. Cominetti, Z. A. E. Waller, M. Searcey, M. A. O'Connell and M. Bochmann, *Inorg. Chem.*, 2017, **56**, 5728–5740.
28 M. Williams, A. I. Green, J. Fernandez-Cestau, D. L. Hughes, M. A. O'Connell, M. Searcey, B. Bertrand and M. Bochmann, *Dalton Trans.*, 2017, **46**, 13397–13408.
29 Y. Jiang, S. Shan, T. Gan, X. Zhang, X. Lu, H. Hu, Y. Wu, J. Sheng and J. Yang, *Biomed. Rep.*, 2014, **2**, 893–897.
30 P. Calamai, S. Carotti, A. Guerri, L. Messori, E. Mini, P. Orioli and G. P. Speroni, *J. Inorg. Biochem.*, 1997, **66**, 103–109.
31 B. D. Glisic, U. Rychlewska and M. I. Djuran, *Dalton Trans.*, 2012, **41**, 6887–6901.
32 (*a*) C. Jacob, G. I. Giles, N. M. Giles and H. Sies, *Angew. Chem., Int. Ed.*, 2003, **42**, 4742–4758; (*b*) B. Noszál, D. Visky and M. Kraszni, *J. Med. Chem.*, 2000, **43**, 2176–2182.
33 (*a*) G. Boscutti, L. Marchio, L. Ronconi and D. Fregona, *Chem. – Eur. J.*, 2013, **19**, 13428–13436; (*b*) T. Zou, C. T. Lum, S. S.-Y. Chui and C.-M. Che, *Angew. Chem., Int. Ed.*, 2013, **52**, 2930–2933.
34 A. Casini, G. Kelter, C. Gabbiani, M. A. Cinellu, G. Minghetti, D. Fregona, H.-H. Fiebig and L. Messori, *J. Biol. Inorg. Chem.*, 2009, **14**, 1139–1149.
35 (*a*) L. Messori, F. Abbate, G. Marcon, P. Orioli, M. Fontani, E. Mini, T. Mazzei, S. Carotti, T. O'Connell and P. Zanello, *J. Med. Chem.*, 2000, **43**, 3541–3548; (*b*) A. Casini, M. A. Cinellu, G. Minghetti, C. Gabbiani, M. Coronnello, E. Mini and L. Messori, *J. Med. Chem.*, 2006, **49**, 5524–5531.
36 L. Ronconi, C. Marzano, P. Zanello, M. Corsini, G. Miolo, C. Macca, A. Trevisan and D. Fregona, *J. Med. Chem.*, 2006, **49**, 1648–1657.
37 S. Spreckelmeyer, C. Orvig and A. Casini, *Molecules*, 2014, **19**, 15584–15610.
38 J. L.-L. Tsai, A. O.-Y. Chan and C.-M. Che, *Chem. Commun.*, 2015, **51**, 8547–8550.
39 (*a*) S. Balasubramanian, L. H. Hurley and S. Neidle, *Nat. Rev. Drug Discovery*, 2011, **10**, 261–275; (*b*) S. Neidle, *J. Med. Chem.*, 2016, **59**, 5987–6011; (*c*) K. Gehring, J. L. Leroy and M. Gueron, *Nature*, 1993, **363**, 561–565; (*d*) H. A. Day, P. Pavlou and Z. A. E. Waller, *Bioorg. Med. Chem.*, 2014, **22**, 4407–4418.
40 D. Monchaud and M. P. Teulade-Fichou, *Org. Biomol. Chem.*, 2008, **6**, 627–636.
41 (*a*) B. Bertrand, L. Stefan, M. Pirrotta, D. Monchaud, E. Bodio, P. Richard, P. Le Gendre, E. Warmerdam, M. H. de Jager, G. M. M. Groothuis, M. Picquet and A. Casini, *Inorg. Chem.*, 2014, **53**, 2296–2303; (*b*) P. Gratteri, L. Massai, E. Michelucci, R. Rigo, L. Messori, M. A. Cinellu, C. Musetti, C. Sissi and C. Bazzicalupi, *Dalton Trans.*, 2015, **44**, 3633–3639.
42 C. Bazzicalupi, M. Ferraroni, F. Papi, L. Massai, B. Bertrand, L. Messori, P. Gratteri and A. Casini, *Angew. Chem., Int. Ed.*, 2016, **55**, 4256–4259.
43 A. De Cian, L. Guittat, M. Kaiser, B. Sacca, S. Amrane, A. Bourdoncle, P. Alberti, M. P. Teulade-Fichou, L. Lacroix and J. L. Mergny, *Methods*, 2007, **42**, 183–195.
44 A. T. Phan and J. L. Mergny, *Nucleic Acids Res.*, 2002, **30**, 4618–4625.
45 J. A. Brazier, A. Shah and G. D. Brown, *Chem. Commun.*, 2012, **48**, 10739–10741.
46 A. Bindoli, M. P. Rigobello, G. Scutari, C. Gabbiani, A. Casini and L. Messori, *Coord. Chem. Rev.*, 2009, **253**, 1692–1707.
47 (*a*) R. Rubbiani, S. Can, I. Kitanovic, H. Alborzinia, M. Stefanopoulou, M. Kokoschka, S. Mönchgesang, W. S. Sheldrick, S. Wölfl and I. Ott, *J. Med. Chem.*, 2011, **54**, 8646–8657; (*b*) E. Shuh, C. Pfluger, A. Citta, A. Folda, M. P. Rigobello, A. Bindoli, A. Casini and F. Mohr, *J. Med. Chem.*, 2012, **55**, 5518–5528; (*c*) B. Bertrand, A. de Almeida, E. P. M. van der Burgt, M. Picquet, A. Citta, A. Folda, M. P. Rigobello, P. Le Gendre, E. Bodio and A. Casini, *Eur. J. Inorg. Chem.*, 2014, 4532–4536.
48 *Programs CrysAlisPro*, Oxford Diffraction Ltd., Abingdon, UK, 2014.
49 G. M. Sheldrick, *Acta Crystallogr., Sect. A: Found. Adv.*, 2015, **71**, 3–8.
50 G. M. Sheldrick, *Acta Crystallogr., Sect. A: Found. Crystallogr.*, 2008, **64**, 112–122 and 2015, C71, 3–8.
51 E. Prince, *International Tables for X-ray Crystallography*, Kluwer Academic Publishers, Dordrecht, 1992, vol. C, pp. 500, 219 and 193.
52 L. J. Farrugia, *J. Appl. Crystallogr.*, 2012, **45**, 849–854.
53 M. Wenzel, B. Bertrand, M.-J. Eymin, V. Comte, J. A. Harvey, P. Richard, M. Groessl, O. Zava, H. Amrouche, P. D. Harvey, P. Le Gendre, M. Picquet and A. Casini, *Inorg. Chem.*, 2011, **50**, 9472–9480.
54 C. Schmidt, B. Karge, R. Misgeld, A. Prokop, R. Franke, M. Brönstrup and I. Ott, *Chem. – Eur. J.*, 2017, **23**, 1869–1880.

